Materials Science Forum Vols. 192-194 (1995) pp. 797-804
online at http://www.scientific.net
© (1995) Trans Tech Publications, Switzerland

Electrochemical Behaviour and Corrosion Resistance of Sputtered W-Ti-N Coatings on Steel Substrates

C.M.A. Brett[1] and A. Cavaleiro[2]

[1] Departamento de Química, Universidade de Coimbra, P-3049 Coimbra, Portugal

[2] Departamento de Engenharia Mecânica, Universidade de Coimbra, P-3049 Coimbra, Portugal

Keywords: Corrosion, Electrochemistry, Hard Coatings, W-Ti-N Coatings, Sputtering, Thin Films

Abstract

The electrochemical behaviour and corrosion resistance of sputtered W-Ti-N coatings on M2 steel substrates in aqueous chloride solution at room temperature has been investigated. The percentage nitrogen and film thickness were varied. Techniques employed include measurement of open-circuit potential, polarisation resistance, response to an applied potential step and electrochemical impedance. Further information was obtained from scanning electron microscopy of the corroded films. The results of the study lead to the conclusion that corrosion occurs preferentially at defects in the sputtered films and that this can be reduced by increased film thickness. Implications for the future use of these films are discussed.

Introduction

A significant amount of research has been done in recent years into the modification of surfaces of metals subject to mechanical solicitations, such as in cutting tools, with a view to increasing their wear resistance. Such modification is often done by coatings produced using physical vapour deposition. Thin film coatings produced by sputtering techniques have the advantage of being thin (1μm - 10μm) which besides reducing the quantity of material required, also reduces residual mechanical stress and problems of differences in thermal expansion coefficients between coating and substrate. Compact and homogeneous coatings, of low porosity, are obtained. Besides wear resistance, a good coating corrosion resistance is important.

Previous recent work on W-C-Co and alumina sputtered coatings on steel substrates has given indications that, in these cases, the corrosion resistance can be better when the films are of amorphous rather than crystalline structure [1]. Other coatings studied recently include Ti-N and Zr-N on AISI304 steel substrates, the former of which was shown to be inert in chloride solutions, any corrosion being a result of the presence of defects in the protecting film, whereas the corrosion of Zr-N was controlled by the oxidation of the nitride to the oxide [2]. Thus Ti-N is a good candidate for corrosion-resistant films, so long as defects can be avoided. Another coating which appears to offer improved corrosion resistance with respect to Ti-N is Ni-Cr-Ti, this conclusion being reached on the basis of corrosion current and polarisation resistance measurements [3].

In this work, the corrosion resistance of M2 steel substrates with W-Ti-N hard coatings produced by dc diode sputtering was studied. These were chosen on the basis of previous results concerning Ti-N and W-C-Co; the films are all crystalline in this case. A number of electrochemical techniques were employed: measurement of open-circuit potential, polarisation resistance, response to potential step and electrochemical impedance. Scanning electron microscopy was used to characterise the morphology.

Experimental

Film/substrate assembly. The substrates were heat-treated cylinders of M2 steel (W 6.4; Mo 5.0; Cr 4.2; V 1.9; C 0.86; Si <0.4; Mn <0.4%) of diameter 1.2cm and thickness 3mm, polished to a mirror-like finish with diamond paste on a polishing table before the sputtering process. Sputtering was carried out with a Hartec dc diode sputtering apparatus. One face of the cylinders was coated in the sputtering vacuum chamber, after a short period of heating and argon ion etching to prepare the substrate surface and improve film adhesion. Deposition was done from a W+10wt.%Ti target, at a power density of 11W cm^{-2}, and a negative substrate bias of 70V. A total gas pressure of 3μbar was employed, the gas being a mixture of argon and nitrogen. Four types of sample were prepared, as shown in Table 1:

Table 1. Characteristics of the four types of film prepared by dc diode sputtering

Type	Film composition (at.%)	Film thickness/μm	N_2 pressure/μbar
1	W(90),Ti(10)	4.5	--
2	W(92),Ti(8)	8.0	--
3	W(52),Ti(14),N(34)	4.5	0.6
4	W(39),Ti(11),N(50)	4.5	1.0

The thickness of the coatings was uniform in each sample and over the ten samples prepared in each deposition experiment; high reproducibility was found between depositions.

Electrochemical cell and instrumentation. A copper wire was attached to the rear face of the coated samples using silver epoxy, and the rear face and edges of the cylinders coated with non-conducting epoxy and varnish, leaving only the coated face exposed. The electrochemical cell also contained a platinum counter electrode and saturated calomel electrode (SCE) as reference. Solutions were usually 0.1M potassium chloride, prepared from analytical grade reagent and distilled, deionised water. Solutions were not de-aerated.

Corrosion potential measurements were done with a Schlumberger SI7151 Computing Multimeter; voltammetric measurements were performed with a PC-controlled EG&G PAR273A potentiostat using PAR Model 352 and Model 270 software. Impedance measurements were done with a Solartron 1250 Frequency Response Analyser coupled to a Solartron 1286 Electrochemical Interface using a 5mV rms perturbation from 65kHz down to 10mHz; experiments were controlled with ZPlot software and simulation was performed with ZSim CNLS software.

Scanning electron microscopy was performed with a Jeol T330 Scanning Electron Microscope with a Tracor Northern Microanalysis Accessory.

Results and Discussion

The results obtained by the different techniques will be presented separately followed by a critical comparison.

Corrosion potential

A typical variation of corrosion potential with time is shown in Fig.1. For all four types of sample there is an initially rapid variation towards negative potentials and which decreases to a low value after about two hours. Some differences between the types of sample are evident. The variations after several hours tend to be in small, abrupt steps which can be attributed to the formation of new pits. Indeed, corrosion potential values registered after several days tend towards that of the substrate (~-0.50V vs. SCE) and there is visual evidence of penetration, with formation of iron oxide. This will be discussed further below in the light of the chemical microanalysis done in conjunction with scanning electron microscopy.

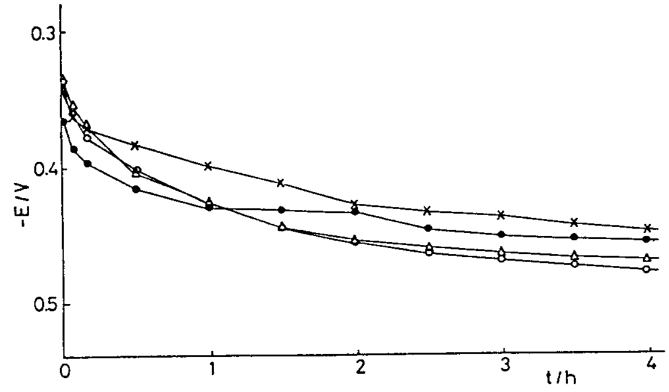

Fig.1 Variation of corrosion potential in 0.1M KCl with time during the first 4 hours: X Type 1; Δ Type 2; O Type 3; ● Type 4.

Examination of the surface of the samples shows the appearance of pits in the surface, less so with the sample with the thicker coating. Thus, the corrosion is non-uniform. The values after 4 hours are also collected in Table 2, together with the values registered after 350h.

Table 2 Corrosion potential and polarisation resistance results

	E_{cor}/V (t=4h)	E_{cor}/V (t=350h)	R_p/Ω cm^2
Type 1	-0.450	-0.549	200
Type 2	-0.470	-0.574	1250
Type 3	-0.478	-0.518	305
Type 4	-0.458	-0.544	435

Linear potential sweep

Two types of potential sweep experiment were undertaken: around the corrosion potential at low scan rate in order to determine the polarisation resistance, R_p, see Table 2, and at higher scan rate over a wide potential range. Fresh samples were used for each measurement.

The polarisation resistance values were obtained at by scanning the potential from E_{cor}-20mV to E_{cor}+20mV at 0.1mV s^{-1} scan rate. They clearly show that film thickness is the most important consideration. For the three types of film of the same thickness, Types 1, 3 and 4, R_p increases with increasing nitrogen content. There is no correlation between the R_p and E_{cor} values. The reason for this is that the film was not ruptured during the course of the R_p measurement (approx. 7 minutes) whereas it was during the 350h corrosion potential measurement. Thus, and importantly, the R_p values give a true indication of the film's resistance to corrosion in the absence of defects or pits, whereas the latter is dependent on these parameters.

Typical cyclic voltammograms are shown in Fig.2. Excursions to the positive potentials shown in the voltammograms result in the formation of pits. Results from these experiments show potential windows, defined as the potential range within which the current is less than 0.5mA, of approximately -1.2V to -0.3V vs. SCE for all four types of sample. There are no striking differences in the cyclic voltammograms for each film type. Additionally, the hysteresis in the anodic part of the voltammogram is less than that with the bare metal substrate [4].

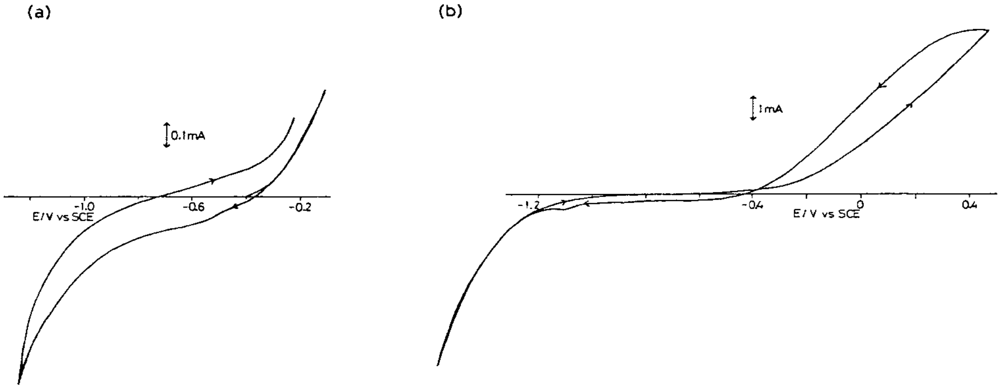

Fig.2 Cyclic voltammograms of Type 4 film on M2 steel substrate after 5 min. immersion; scan rate 10mV s^{-1}: (a) 1st scan (b) 5th scan.

Potential step

Potential steps were applied from -0.5V to -0.2V vs. SCE. The initial value was chosen as being close to the corrosion potential, and the final value in the pitting region. It can be seen from Fig.3 that the order of inertness of the samples is different from that obtained by the techniques described above. This gives indications that the cause of corrosion is actually defects in the film. After about 5s the current falls to an apparently constant value, Fig.3a. However, long-time studies indicate that the current increases linearly with time, Fig. 3b, which can be attributed to formation of iron hydroxide either in one dimension perpendicular to the substrate/film surface or due to two-dimensional lateral growth [5]. Interestingly, the slopes of the I vs. t plots are almost equal and are independent of the film type. This will be further discussed in conjunction with the results from scanning electron microscopy examination of the surface morphology.

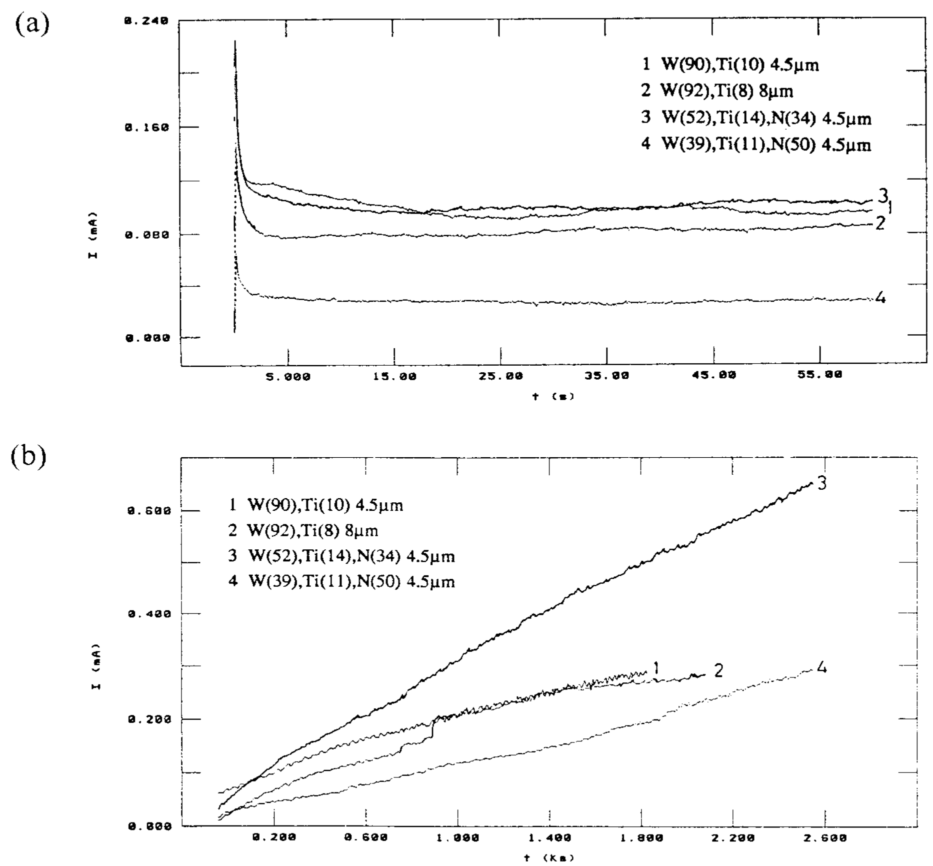

Fig.3 Chronoamperometry after potential step from -0.5V to -0.2V vs. SCE
(a) Initial variation (b) Long-time variation.

Electrochemical impedance

Impedance spectra were recorded at potentials corresponding to the open-circuit potential at the beginning of the experiment and at an applied potential of -0.3V vs. SCE. These all had the form of a depressed semicircle together with transmission-line characteristics for a diffusion-controlled process (finite Warburg impedance) at low frequency. An example is given in Fig.4. The effect of applying a more positive potential was to reduce the resistance values; the form of the plots remained the same. Such a behaviour is not unexpected for a film with slight porosity. For modelling the substrate/film/solution assembly, it is logical that the equivalent circuit should contain an *RC* parallel combination for the film/solution interface and a resistance corresponding to the bulk film. Given the heterogeneous nature of the film and porosity, it is also likely that two *RC* parallel combinations are necessary for this interface, and with constant phase element characteristics. This in fact works; the results of the simulation are also shown in Fig.4.

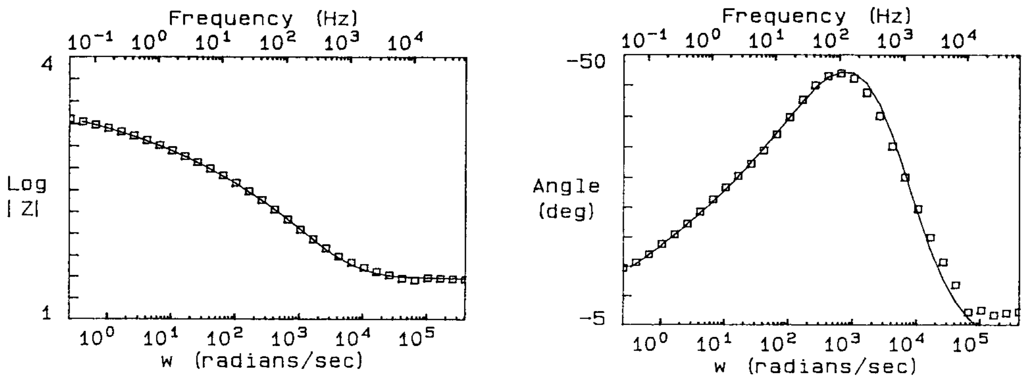

Fig.4 Bode plots of electrochemical impedance of Type 3 film at -0.35V;
□ experimental points; —— simulation.

Comparison of results obtained and scanning electron microscopy

An understanding of the electrochemical results is aided by consideration of the coating structure and morphology. The structure of the coatings is crystalline with Ti substituting W in the W metal lattice; N, which improves the mechanical properties, is present predominantly in interstitial sites. Scanning electron microscopy shows some roughness and porosity in the surface morphology of the freshly-produced coatings which is greater the longer the etching time by argon ions (some etching is necessary to ensure good film adhesion to the substrate). Cross-sectional examination shows that besides the pores, which in general do not penetrate down to the substrate, there is a tendency for columnar structural formations in the film with the possibility of the occasional fissure reaching to the substrate itself. This is more evident for W-Ti films without nitrogen which typically have a

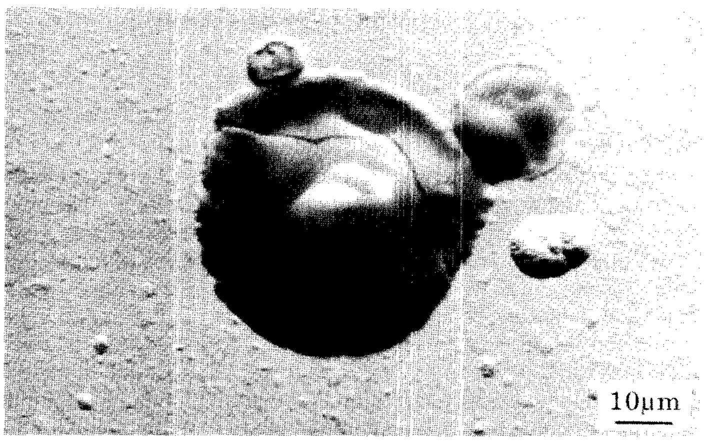

Fig.5 Scanning electron microscopy of the surface of a Type 3 film in the zone of pit formation.

Type 1 morphology [6]; W-Ti-N films have a more compact Type T microstructure with less well-defined columns. The polarisation resistance results, which probe the film's behaviour in the absence of pitting, are in agreement with these observations. This technique is thus an excellent probe of the corrosion resistance of "perfect" films.

An example of scanning electron microscopy of the corroded surface is shown in Fig.5. It gives evidence of how the corrosion process begins. The film is lifted and a skin, which is predominantly iron hydroxide, forms over the place where pitting occurs, and probably acts as a semi-permeable membrane. This is then eventually ruptured allowing easier access to oxygen and protons, and the corrosion becomes faster. Microanalysis of the bare surface of the M2 steel exposed below shows that it is poorer in iron content than in the other elements of the alloy; this is also found in corrosion studies of the bare M2 steel substrate. With respect to the oxide growth mechanism and in the light of the potential step results, examination of the micrographs suggests that both 1-D perpendicular and 2-D lateral growth of the oxide film occur.

These considerations lead to the conclusion that the observed electrochemical and impedance behaviour can be rationalised in terms of electrolyte penetration through the film. Effects of localised corrosion are observed macroscopically, as is some lateral corrosion of the substrate beneath the coating. Microscopic examination of the surface before and after electrochemical experiments suggests that the corrosion rate of the coating itself in the absence of defects or pores is low. These aspects are currently being further investigated. Differences in the results obtained between the various techniques can be explained in this way. It suggests that one of the main preoccupations in the fabrication of these sputtered coatings must be the production of films which are free of microscopic defects, including avoiding the trapping of gas beneath the coating which increases mechanical tensions and reduces adhesion, probably also leading to an increased probability of corrosion.

Conclusions

A number of electrochemical techniques and scanning electron microscopy plus chemical microanalysis have been used to examine the corrosion of W-Ti and W-Ti-N crystalline coatings on M2 steel substrates. Results indicate that the major factor in reducing corrosion is increased film thickness; increasing the nitrogen content also reduces corrosion, but to a lesser extent. This is particularly shown through polarisation resistance values. Pitting, which probably initiates in defects in the as-produced films, once it occurs dominates the electrochemical behaviour. This demonstrates the importance of producing films which are defect-free on a microscopic scale.

Acknowledgement

The Junta Nacional de Investigação Científica, Portugal (JNICT) is thanked for financial support through project PBIC/C/CTM/1383/92.

References

[1] C.M.A. Brett and M.T. Vieira, Abstracts of 44th Meeting of ISE, Berlin, 1993.
[2] R. Brown, M.N. Alias and R. Fontana, Surf. Coat. Technol. **62**, 467 (1993).
[3] I. Montero, C. Jiménez and J. Perrière, Surf. Sci. **251/252**, 1038 (1991).
[4] C.M.A. Brett and P.I.C. Melo, in preparation.
[5] J.W. Schultze, M.M. Lohrengel and D. Ross, Electrochim. Acta **28**, 973 (1983).
[6] J.A. Thornton, Ann. Rev. Mater. Sci. 7,239(1977).